Modelling, validation and adaptive PID control with pitch moment rejection of active suspension system for reducing unwanted vehicle motion in longitudinal direction

Article *in* International Journal of Vehicle Systems Modelling and Testing · January 2010

DOI: 10.1504/IJVSMT.2010.038036

CITATIONS
25

READS
3,225

4 authors:

Fauzi Ahmad
Technical University of Malaysia Malacca
35 PUBLICATIONS **257** CITATIONS
SEE PROFILE

Khisbullah Hudha
National Defence University of Malaysia
151 PUBLICATIONS **1,154** CITATIONS
SEE PROFILE

Fitrian Imaduddin
Universitas Sebelas Maret
119 PUBLICATIONS **1,238** CITATIONS
SEE PROFILE

Hishamuddin Jamaluddin
Southern University College, Johor Bahru
119 PUBLICATIONS **2,114** CITATIONS
SEE PROFILE

Modelling, validation and adaptive PID control with pitch moment rejection of active suspension system for reducing unwanted vehicle motion in longitudinal direction

Fauzi Ahmad*, Khisbullah Hudha and Fitrian Imaduddin

Center of Vehicle Research and Development (CeVReD),
Faculty of Mechanical Engineering,
Universiti Teknikal Malaysia Melaka (UTeM),
Karung Berkunci 1200, Hang Tuah Jaya,
Ayer Keroh 75450 Melaka, Malaysia
E-mail: fauzi_ahmad1984@yahoo.com.my
E-mail: khisbullah@utem.edu.my
E-mail: fimaduddin@yahoo.com
*Corresponding author

Hishammudin Jamaluddin

Faculty of Mechanical Engineering,
Universiti Teknologi Malaysia (UTM),
81310 UTM Skudai, Johor, Malaysia
E-mail: hishamj@fkm.utm.my

Abstract: This paper provides a detailed derivation of a full vehicle model, which may be used to simulate the behaviour of a vehicle in longitudinal direction. The 14 degrees of freedom (14-DOF) vehicle model is integrated with an analytical tyre dynamics using Calspan tyre model. The full vehicle model was validated experimentally with an instrumented experimental vehicle based on the driver input from brake or throttle pedals. Several transient handling tests were performed, namely sudden acceleration and sudden braking test. Comparisons of the experimental result and model response with sudden braking and throttling imposed motion are made. The results of model validation show that the trends between simulation results and experimental data are almost similar with acceptable error. An adaptive PID control strategy was implemented on the validated full vehicle model to reduce unwanted vehicle motions in longitudinal direction during sudden braking and throttling manoeuvre. The results show that the proposed control structure is able to significantly improve the dynamic performance of the vehicle during sudden braking and sudden acceleration under various conditions.

Keywords: active suspension; dive and squat; 14 DOF; vehicle model; adaptive PID; pitch moment rejection.

Reference to this paper should be made as follows: Ahmad, F., Hudha, K., Imaduddin, F. and Jamaluddin, H. (2010) 'Modelling, validation and adaptive PID control with pitch moment rejection of active suspension system for reducing unwanted vehicle motion in longitudinal direction', *Int. J. Vehicle Systems Modelling and Testing*, Vol. 5, No. 4, pp.312–346.

Biographical notes: Fauzi Ahmad received his BEng and MSc from the Department of Mechanical Engineering Automotive, Universiti Teknikal Malaysia Melaka (UTeM). He is currently a Lecturer at the Department of Automotive, Faculty of Mechanical Engineering, Universiti Teknikal Malaysia Melaka (UTeM), Melaka, Malaysia. His research interests include tyre modelling, vehicle ride and handling, pneumatic system modelling and adaptive PID control. His current research project is to develop a 3-DOF motion platform for vehicle dynamic simulator.

Khisbullah Hudha received his BEng of Mechanical Design from Bandung Institute of Technology (ITB) Indonesia, his MSc from the Department of Engineering Production Design, Technische Hoogeschool Utrecht, the Netherlands and his PhD ('Intelligent vehicle dynamics control using magnetorheological damper') from Malaysia University of Technology (UTM). His research interests include modelling, identification and force tracking control of semi-active damper, evaluation of vehicle ride and handling, electronic chassis control system design and intelligent control. He is currently attached with Universiti Teknikal Malaysia Melaka (UTeM).

Fitrian Imaduddin received his BEng in Engineering Physics from Institut Teknologi Sepuluh Nopember (ITS) Indonesia and his MSc in Mechanical Engineering from Universiti Teknikal Malaysia Melaka (UTeM). His research interests include modelling and control of mechatronic systems. He is currently a Research Assistant at the Center of Vehicle Research and Development (CeVReD).

Hishamuddin Jamaluddin received his BSc, MSc and PhD at the Department of Control Engineering, Sheffield University, UK. He is currently a Professor at the Department of Applied Mechanics, Faculty of Mechanical Engineering, Universiti Teknologi Malaysia, Johor, Malaysia. His research interests include non-linear system modelling, system identification, neural networks, adaptive fuzzy models, genetic algorithm, neuro-fuzzy and active force control.

1 Introduction

It is deemed necessary and useful to isolate disturbance elements that are prevalent in many mechanical systems. A clear example can be seen in an automotive system in which the passengers of a car should ideally be isolated from vibration or shaking effects of the car's body when the car hits a bump, cornering and braking. Referring to the characteristic of the vehicle movement in longitudinal direction, the vehicle will dive forward when brake is applied. This is due to the fact that, inertia will cause a shift in the vehicle's centre of gravity and weight will be transferred from the rear tyres to the front tyres. Similarly, the vehicle will squat to the rear when throttle input is applied. This is due to the weight transfer from the front to the rear. Both dive and squat are unwanted vehicle motions known as vehicle pitching (Ahmad et al., 2008a, 2008b; Fenchea, 2008). This motion will cause the vehicle to become unstable, lack handling performance, out of control and moreover may cause an accident (Bahouth, 2005). Although this problem is severe, the common passive suspension is unable to generate energy to suppress the weight transfers that causes moment. It is because the spring damper elements are

generally fixed and are chosen based on the design requirement of the vehicle (Priyandoko and Mailah, 2005).

To solve these problems, considerable amount of works have been carried out both theoretically and experimentally (Alleyne and Heddrick, 1995; Lin and Kanellakopoulos, 1997). Through the combination of mechanical, electrical and hydraulic components, a wide range of controllable suspension systems have been developed varying in cost, sophistication and effectiveness. In general, these systems can be classified into three categories: semi-active suspensions (Gao et al., 2006; Hudha et al., 2003; Yoshimura et al., 1997a), active anti-roll bars (Sampson et al., 2000; Sampson, 2002) and active suspensions (Weeks et al., 2000; Yoshimura et al., 2001; Sam and Osman, 2005). A semi active suspension is a passive system with controlled components usually the orifice or the fluid viscosity, which is able to adjust the stiffness of the damper. The active anti-roll bar system consists of an anti-roll bar mounted in the body and two actuators on each axle to cancel out the unwanted body motion, while the active suspension system is a controllable suspension that has the ability to add energy into the system, as well as store and dissipate it.

Recently, the investigation of active suspension systems for car models has increased significantly because they offer better ride comfort to passengers of high-speed ground transportation compared with passive and semi-active suspension systems. The research on active suspension systems is based on optimal control theory on the assumption that the car model is described by a linear or approximately linear system whose performance index is given by a quadratic form of the state variables (Sampson and Cebon 2003a, 2003b; Karnopp, 1995; Sam and Osman, 2006). However, non-linear and intelligent active suspension systems have been proposed for complicated models with strong non-linearity and uncertainty. Numerical and experimental results have shown that active suspension systems result with relatively more satisfactory performance, but need larger loads to achieve active control, compared with the linear active suspension systems (Yoshimura et al., 2003; Yoshimura and Watanabe, 2003; Kruczek and Stribrsky, 2004; Toshio and Itaru, 2005). Some of the studies used 4-DOF vehicle model (Campos et al., 1999; Vaughan et al., 2003), 7-DOF vehicle model has been investigated by Ikanega et al. (2000) and Zhang et al. (2004).

The study on the effectiveness of an active suspension system on real vehicle has been lead by Lotus Company in the early 1980s. The company proposed a hydraulic active suspension system as a means to improve cornering for racing cars and came out with a new electro-hydraulic active suspension that is used in Lotus Excel model in 1985, but this was never offered to public (Holford et al., 2001). Six years after that, Nissan Motor Company produced a new type of luxury car that included traction control system and the world's first full-active suspension (FAS). It used hydraulic actuators as the controllable suspension and used ten sensors to counteract body lean, nose lift and nose dive, and fore/aft pitch on wavy surfaces (March and Shim, 2007). Besides that, Mercedes Company used hydraulic system to eliminate body roll called active body control system (ABC). In this application, the conventional spring-damper unit is mounted in series with the fluid chamber. When the car is cornering, the springs on the outer side of the corner will be compressed and at the same time the fluid chamber will be filled to compensate for the compression of the spring. Similarly BMW company also used a hydraulic system to prevent body roll namely dynamic drive. The hydraulic system is used as the element in the anti roll bar that can supply torque to each side of the anti roll bar (Fischer and Isermann, 2004).

Since hydraulic system is widely used as the active suspension, Citroen Company developed an active suspension system differently by using the combination of the hydraulic and pneumatic system named hydractive suspension system implemented in Citreon Xantia Model 1989 (Ruotsalainen et al., 2006). Furthermore, Bose known for its high-performance audio products, has developed an active suspension system which uses linear electric motors that replace the conventional spring-damper unit to produce the force required for eliminating body roll and pitch. The improvement in ride quality and the ability to suppress roll and pitch comes at the expense of energy consumption. However, in contrast to a hydraulic active suspension the linear motor can also function as a generator. That is, the motor has to produce a force in the opposite direction of its velocity, and energy can be generated where normally it would be dissipated by a conventional damper (Wang and Smith, 2002).

The extensive research on active suspension has resulted with many control strategies. These control strategies may be loosely grouped into linear, non-linear, hybrid and intelligent control approaches. The linear control strategies is mainly based on the optimal control theory such as LQR, LQG, LTR and H-infinity and are capable of minimising a defined performance index. Application of the LQR method in active suspension system has been proposed by Hrovat (1991), Sam et al. (2000) and Su et al. (2008). The non-linear control strategies that have been applied in controlling active suspension are fuzzy logic control used by Toshio and Itaru (2005), Yoshimura et al. (1997b) and sliding mode control (SMC) by Park and Kim (1998), Decarlo et al. (1988) and Sam and Osman (2005). In terms of hybrid control strategies, PID fuzzy logic neural network (NN) and genetic algorithm (GA) have been applied to the active suspension system such as GA-based PID proposed by Garg and Kumar (2002) and sliding mode fuzzy control technique proposed by Ting et al. (1995). Other intelligent control strategies have been proposed such as fuzzy reasoning disturbance observer (Toshio and Itaru, 2005) and adaptive fuzzy active force control (Mailah and Priyandoko, 2007).

Sparked by technological sophistication nowadays, a pneumatically actuated active suspension (PAAS) system is proposed. The proposed PAAS system is used to minimise the effects of unwanted pitch and vertical body motions of the vehicle in the presence of braking or throttle input from the driver. Like those stated, the proposed active suspension system is the system in which the passive suspension system is augmented by pneumatic actuators that supply additional external forces. The system was developed by using four units pneumatic system that were installed between lower arms and vehicle body parallel with passive suspension. The reason of using pneumatic system due to the cheap cost for implementing in a real vehicle, the availability of air without cost to pay and the compressibility of air that can be used as the medium to transmit force. The proposed control strategy for the PAAS system is the combination of adaptive PID (APID)-based feedback control and pitch moment rejection-based feed forward control (Stilwel and Rugh, 1999; Lee et al., 2001; Sedaghati, 2006; Fialho and Balas, 2002). Feedback control is used to minimise unwanted body pitch motions, while the feed forward control is intended to reduce the unwanted weight transfer during braking and throttle manoeuvres. The forces produced by the proposed control structure are used as the target forces by the four unit pneumatic actuators. The reason for using adaptive control-based PID controller is because the PID controller has already proven effective in many applications where it is easy to maintain and easy to implement in the Online Famos.

The proposed control structure is implemented on a validated full vehicle model. The full vehicle model can be approximately described as a 14-DOF system subject to excitation from braking and throttling inputs. It consists of 7-DOF vehicle ride model and 7-DOF vehicle handling model coupled with Calspan tyre model (Kasprzak et al., 2006; Kasprzak and Gentz, 2006; Kadir et al., 2008; Ahmad et al., 2009; Hudha et al., 2009). MATLAB-SIMULINK software was chosen as a computer simulation tool used to simulate the vehicle dynamics behaviour and evaluate the performance of the control structure. In order to verify the effectiveness of the proposed controller, passive system and active system with PID controller without pitch moment rejection were selected as the benchmark.

This paper is organised as follows: the first section contains the introduction and the review of some related works, followed by mathematical derivations of a 14-DOF full vehicle model with Calspan tyre model in the second section. The third section presents the proposed control structure for the PAAS system. The following section explains about the validation of 14-DOF vehicle model with the data obtained from instrumented experimental vehicle. The fifth section presents the performance evaluation of the proposed control structure. The last section contains some conclusion.

2 Full vehicle model with Calspan tyre model

The full-vehicle model of the passenger vehicle considered in this study consists of a single sprung mass (vehicle body) connected to four unsprung masses and is represented as a 14-DOF system. The sprung mass is represented as a plane and is allowed to pitch, roll and yaw as well as to displace in vertical, lateral and longitudinal directions. The unsprung masses are allowed to bounce vertically with respect to the sprung mass. Each wheel is also allowed to rotate along its axis and only the two front wheels are free to steer.

2.1 Modelling assumptions

Some of the modelling assumptions considered in this study are as follows: the vehicle body is lumped into a single mass which is referred to as the sprung mass, aerodynamic drag force is ignored, and the roll centre is coincident with the pitch centre and located at just below body centre of gravity. The suspensions between the sprung mass and unsprung masses are modelled as passive viscous dampers and spring elements. Rolling resistance due to passive stabiliser bar and body flexibility are neglected. The vehicle remains grounded at all times and the four tyres never lost contact with the ground during manoeuvrings. A 4 degrees tilt angle of the suspension system towards vertical axis is neglected ($\cos 4 = 0.998 \approx 1$). Tyre vertical behaviour is represented as a linear spring without damping, whereas the lateral and longitudinal behaviours are represented with Calspan model. Steering system is modelled as a constant ratio and the effect of steering inertia is neglected.

2.2 Vehicle ride model

The vehicle ride model is represented as a 7-DOF system. It consists of a single sprung mass (car body) connected to four unsprung masses (front-left, front-right, rear-left and

rear-right wheels) at each corner. The sprung mass is free to heave, pitch and roll while the unsprung masses are free to bounce vertically with respect to the sprung mass. The suspensions between the sprung mass and unsprung masses are modelled as passive viscous dampers and spring elements. The tyres are modelled as simple linear springs without damping. For simplicity, all pitch and roll angles are assumed to be small. A similar model was used by Ikanega et al. (2000).

Referring to Figure 1, the force balance on sprung mass is given as:

$$F_{fl} + F_{fr} + F_{rl} + F_{rr} + F_{pfl} + F_{pfr} + F_{prl} + F_{prr} = m_s \ddot{Z}_s \tag{1}$$

where

F_{fl} suspension force at front left corner

F_{fr} suspension force at front right corner

F_{rl} suspension force at rear left corner

F_{rr} suspension force at rear right corner

m_s sprung mass weight

$\ddot{Z}_s$ sprung mass acceleration at body centre of gravity

F_{pfl} pneumatic actuator forces at front left corners

F_{pfr} pneumatic actuator forces at front right corners

F_{prl} pneumatic actuator forces at rear left corners

F_{prr} pneumatic actuator forces at rear right corners.

Figure 1 A 14-DOF Full vehicle ride and handling model

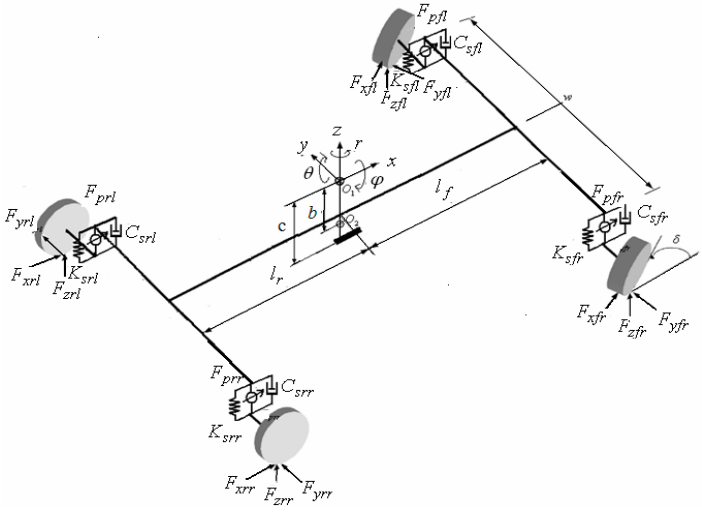

The suspension force at each corner of the vehicle is defined as the sum of the forces produced by suspension components namely spring force and damper force as the following:

$$
\begin{aligned}
F_{fl} &= K_{s,fl}\left(Z_{u,fl} - Z_{s,fl}\right) + C_{s,fl}\left(\dot{Z}_{u,fl} - \dot{Z}_{s,fl}\right) \\
F_{fr} &= K_{s,fr}\left(Z_{u,fr} - Z_{s,fr}\right) + C_{s,fr}\left(\dot{Z}_{u,fr} - \dot{Z}_{s,fr}\right) \\
F_{rl} &= K_{s,rl}\left(Z_{u,rl} - Z_{s,rl}\right) + C_{s,rl}\left(\dot{Z}_{u,rl} - \dot{Z}_{s,rl}\right) \\
F_{rr} &= K_{s,rr}\left(Z_{u,rr} - Z_{s,rr}\right) + C_{s,rr}\left(\dot{Z}_{u,rr} - \dot{Z}_{s,rr}\right)
\end{aligned}
\tag{2}
$$

where

$K_{s,fl}$ front left suspension spring stiffness

$K_{s,fr}$ front right suspension spring stiffness

$K_{s,rr}$ rear right suspension spring stiffness

$K_{s,rl}$ rear left suspension spring stiffness

$C_{s,fr}$ front right suspension damping

$C_{s,fl}$ front left suspension damping

$C_{s,rr}$ rear right suspension damping

$C_{s,rl}$ rear left suspension damping

$Z_{u,fr}$ front right unsprung masses displacement

$Z_{u,fl}$ front left unsprung masses displacement

$Z_{u,rr}$ rear right unsprung masses displacement

$Z_{u,rl}$ rear left unsprung masses displacement

$Z_{u,fr}$ front right unsprung masses velocity

$Z_{u,\mathrm{fl}}$ front left unsprung masses velocity

$Z_{u,rr}$ rear right unsprung masses velocity

$Z_{u,rl}$ rear left unsprung masses velocity.

The sprung mass position at each corner can be expressed in terms of bounce, pitch and roll given by:

$$
\begin{aligned}
Z_{s,fl} &= Z_s - a\sin\theta + 0.5w\sin\phi \\
Z_{s,fr} &= Z_s - a\sin\theta - 0.5w\sin\phi \\
Z_{s,rl} &= Z_s + b\sin\theta + 0.5w\sin\phi \\
Z_{s,rr} &= Z_s + a\sin\theta - 0.5w\sin\phi
\end{aligned}
\tag{3}
$$

It is assumed that all angles are small, therefore, equation (3) becomes:

$$
\begin{aligned}
Z_{s,fl} &= Z_s - a\theta + 0.5w\phi \\
Z_{s,fr} &= Z_s - a\theta - 0.5w\phi \\
Z_{s,rl} &= Z_s + b\theta + 0.5w\phi \\
Z_{s,rr} &= Z_s + a\theta - 0.5w\phi
\end{aligned}
\tag{4}
$$

where

lf distance between front of vehicle and centre of gravity of sprung mass

lr distance between rear of vehicle and centre of gravity of sprung mass

w track width

m vehicle mass

θ pitch angle at body centre of gravity

ϕ roll angle at body centre of gravity

$Z_{s,fl}$ front left sprung mass displacement

$Z_{s,fr}$ front right sprung mass displacement

$Z_{s,rl}$ rear left sprung mass displacement

$Z_{s,rr}$ rear right sprung mass displacement.

By substituting equation (4) and its derivative (sprung mass velocity at each corner) into equation (2) and the resulting equations are then substituted into equation (1), the following equation is obtained:

$$\begin{aligned} m_s\ddot{Z}_s = & -2\left(K_{s,f}+K_{s,r}\right)Z_s - 2\left(C_{s,f}+C_{s,r}\right)\dot{Z}_s + 2\left(aK_{s,f}-bC_{s,r}\right)\theta \\ & + 2\left(aC_{s,f}-bC_{s,r}\right)\dot{\theta} + K_{sf}Z_{u,fl} + C_{s,f}\dot{Z}_{u,fl} + K_{sf}Z_{u,fr} \\ & + C_{s,f}\dot{Z}_{u,fr}K_{sr}Z_{u,rl} + C_{s,r}\dot{Z}_{u,rl} + K_{sr}Z_{u,rr} + C_{s,r}\dot{Z}_{u,rr} \\ & + F_{pfl} + F_{pfr} + F_{prl} + F_{prr} \end{aligned} \tag{5}$$

where

$\dot{\theta}$ pitch rate at body centre of gravity

Z_s sprung mass displacement at body centre of gravity

$\dot{Z}_s$ sprung mass velocity at body centre of gravity

$K_{s,f}$ spring stiffness of front suspension *($K_{s,fl} = K_{s,fr}$)*

$K_{s,r}$ spring stiffness of rear suspension *($K_{s,rl} = K_{s,rr}$)*

$C_{s,f} = C_{s,fl} = C_{s,fr}$ damping constant of front suspension

$C_{s,r} = C_{s,rl} = C_{s,rr}$ damping constant of rear suspension.

Similarly, moment balance equations are derived for pitch θ and roll φ, and are given as:

$$\begin{aligned} I_{yy}\ddot{\theta} = & 2\left(aK_{s,f}-bK_{s,r}\right)Z_s + 2\left(aC_{s,f}-bC_{s,r}\right)\dot{Z}_s - 2\left(a^2K_{s,f}+b^2K_{s,r}\right)\theta \\ & -2\left(a^2C_{s,f}+b^2C_{s,r}\right)\dot{\theta} - aK_{s,f}Z_{u,fl} - aC_{s,f}\dot{Z}_{u,fl} - aK_{s,f}Z_{u,fr} \\ & -aC_{s,f}\dot{Z}_{u,fr} + bK_{s,r}Z_{u,rl} + bC_{s,r}\dot{Z}_{u,rl} + bK_{s,r}Z_{u,rr} + bC_{s,r}\dot{Z}_{u,rr} \\ & -\left(F_{pfl}+F_{pfr}\right)l_f + \left(F_{prl}+F_{prr}\right)l_r \end{aligned} \tag{6}$$

$$\begin{aligned} I_{xx}\ddot{\phi} = & -0.5w^2\left(K_{s,f}+K_{s,r}\right)\phi - 0.5w^2\left(C_{s,f}+C_{s,r}\right)\dot{\phi} + 0.5wK_{s,f}Z_{u,fl} \\ & + \ 0.5wC_{s,f}\dot{Z}_{u,fl} - 0.5wK_{s,f}Z_{u,fr} - 0.5wC_{s,f}\dot{Z}_{u,fr} \\ & + \ 0.5wK_{s,r}Z_{u,rl} + 0.5wC_{s,r}\dot{Z}_{u,rl} - 0.5wK_{s,r}Z_{u,rr} - 0.5wC_{s,r}\dot{Z}_{u,rr} \\ & + \ \left(F_{pfl}+F_{prl}\right)\frac{w}{2} - \left(F_{pfr}+F_{prr}\right)\frac{w}{2} \end{aligned} \tag{7}$$

where

$\ddot{\theta}$ pitch acceleration at body centre of gravity

$\ddot{\phi}$ roll acceleration at body centre of gravity

I_{xx} roll axis moment of inertia

I_{yy} pitch axis moment of inertia

w wheel base of sprung mass.

By performing force balance analysis at the four wheels, the following equations are obtained:

$$\begin{aligned} m_u\ddot{Z}_{u,fl} = & K_{s,f}Z_s + C_{s,f}\dot{Z}_s - aK_{s,f}\theta - aC_{s,f}\dot{\theta} + 0.5wK_{s,f}\phi \\ & + \ 0.5wC_{s,f}\dot{\phi} - \left(K_{s,f}+K_t\right)Z_{u,fl} - C_{s,f}\dot{Z}_{u,fl} + K_tZ_{r,fl} - F_{pfl} \end{aligned} \tag{8}$$

$$\begin{aligned} m_u\ddot{Z}_{u,fr} = & K_{s,f}Z_s + C_{s,f}\dot{Z}_s - aK_{s,f}\theta - aC_{s,f}\dot{\theta} - 0.5wK_{s,f}\phi \\ & - \ 0.5wC_{s,f}\dot{\phi} - \left(K_{s,f}+K_t\right)Z_{u,fr} - C_{s,f}\dot{Z}_{u,fr} + K_tZ_{r,fr} - F_{pfr} \end{aligned} \tag{9}$$

$$\begin{aligned} m_u\ddot{Z}_{u,rl} = & K_{s,r}Z_s + C_{s,r}\dot{Z}_s + bK_{s,r}\theta + bC_{s,r}\dot{\theta} + 0.5wK_{s,r}\phi \\ & + \ 0.5wC_{s.r}\dot{\phi} - \left(K_{s,r}+K_t\right)Z_{u,rl} - C_{s,r}\dot{Z}_{u,rl} + K_tZ_{r,rl} - F_{prl} \end{aligned} \tag{10}$$

$$\begin{aligned} m_u\ddot{Z}_{u,rr} = & K_{s,r}Z_s + C_{s,r}\dot{Z}_s + aK_{s,r}\theta + bC_{s,r}\dot{\theta} - 0.5wK_{s,r}\phi \\ & - \ 0.5wC_{s,r}\dot{\phi} - \left(K_{s,r}+K_t\right)Z_{u,rr} - C_{s,r}\dot{Z}_{u,rr} + K_tZ_{r,rr} - F_{prr} \end{aligned} \tag{11}$$

where

$\ddot{Z}_{u,fr}$ front right unsprung masses acceleration

$\ddot{Z}_{u,fl}$ front left unsprung masses acceleration

$\ddot{Z}_{u,rr}$ rear right unsprung masses acceleration

$\ddot{Z}_{u,rl}$ rear left unsprung masses acceleration

$Z_{r,fr} = Z_{r,fl} = Z_{r,rr} = Z_{r,rl}$ road profiles at front left, front right, rear right and rear left tyres respectively.

2.3 Vehicle handling model

The handling model employed in this paper is a 7-DOF system as shown in Figure 2. It takes into account three degrees of freedom for the vehicle body in lateral and longitudinal motions as well as yaw motion *(r)* and one degree of freedom due to the rotational motion of each tyre. In vehicle handling model, it is assumed that the vehicle is moving on a flat road. The vehicle experiences motion along the longitudinal *x*-axis and the lateral *y*-axis, and the angular motions of yaw around the vertical *z*-axis. The motion in the horizontal plane can be characterised by the longitudinal and lateral accelerations, denoted by a_x and a_y respectively, and the velocities in longitudinal and lateral direction, denoted by v_x and v_y, respectively.

Figure 2 A 7-DOF vehicle handling model

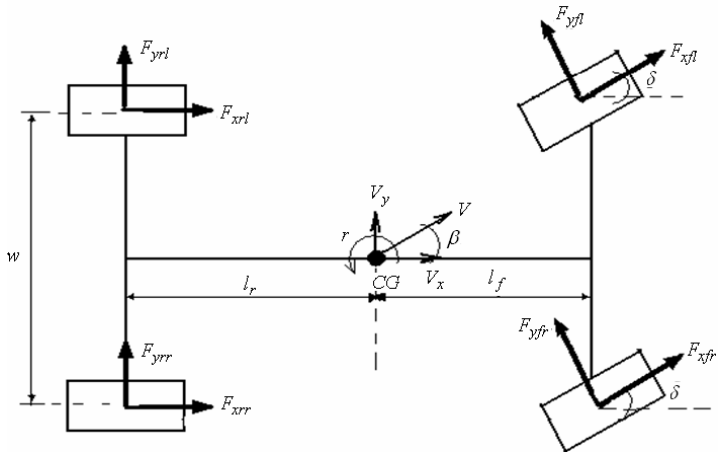

Acceleration in longitudinal *x*-axis is defined as:

$$\dot{v}_x = a_x + v_y \dot{r} \tag{12}$$

By summing all the forces in *x*-axis, longitudinal acceleration can be defined as:

$$a_x = \frac{F_{xfl}\cos\delta + F_{yfl}\sin\delta + F_{xfr}\cos\delta + F_{yfr}\sin\delta + F_{xrl} + F_{xrr}}{m_t} \tag{13}$$

Similarly, acceleration in lateral y-axis is defined as:

$$\dot{v}_y = a_y - v_x \dot{r} \tag{14}$$

By summing all the forces in lateral direction, lateral acceleration can be defined as:

$$a_y = \frac{F_{yfl}\cos\delta - F_{xfl}\sin\delta + F_{yfr}\cos\delta - F_{xfr}\sin\delta + F_{yrl} + F_{yrr}}{m_t} \tag{15}$$

where F_{xij} and F_{yij} denote the tyre forces in the longitudinal and lateral directions, respectively, with the index *(i)* indicating front *(f)* or rear *(r)* tyres and index *(j)* indicating

left *(l)* or right *(r)* tyres. The steering angle is denoted by δ, the yaw rate by $\dot{r}$ and m_t denotes the total vehicle mass. The longitudinal and lateral vehicle velocities v_x and v_y can be obtained by the integration of v_x and v_y. They can be used to obtain the side slip angle, denoted by α. Thus, the slip angle of front and rear tyres are found as:

$$\alpha_f = \tan^{-1}\left(\frac{v_y + L_f r}{v_x}\right) - \delta_f \tag{16}$$

and

$$\alpha_r = \tan^{-1}\left(\frac{v_y - L_f r}{v_x}\right) \tag{17}$$

where, a_f and a_r are the side slip angles at front and rear tyres respectively while l_f and l_r are the distance between front and rear tyre to the body centre of gravity respectively.

To calculate the longitudinal slip, longitudinal component of the tyre velocity should be derived. The front and rear longitudinal velocity component is given by:

$$v_{wxf} = V_{tf} \cos\alpha_f \tag{18}$$

where the speed of the front tyre is:

$$V_{tf} = \sqrt{\left(v_y + L_f r\right)^2 + v_x^2} \tag{19}$$

The rear longitudinal velocity component is:

$$v_{wxr} = V_{tr} \cos\alpha_r \tag{20}$$

where the speed of the rear tyre is:

$$V_{tr} = \sqrt{\left(v_y + L_r r\right)^2 + v_x^2} \tag{21}$$

Then, the longitudinal slip ratio of front tyre:

$$S_{af} = \frac{v_{wxf} - \omega_f R_w}{v_{wxf}} \text{ under braking conditions} \tag{22}$$

The longitudinal slip ratio of rear tyre is:

$$S_{ar} = \frac{v_{wxr} - \omega_r R_w}{v_{wxr}} \text{ under braking conditions} \tag{23}$$

where ω_r and ω_f are angular velocities of rear and front tyres, respectively and R_w, is the wheel radius. The yaw motion is also dependent on the tyre forces F_{xij} and F_{yij} as well as on the self-aligning moments, denoted by M_{zij} acting on each tyre:

$$\ddot{r} = \frac{1}{J_z}\begin{bmatrix} \frac{w}{2}F_{xfl}\cos\delta - \frac{w}{2}F_{xfr}\cos\delta + \frac{w}{2}F_{xrl} - \frac{w}{2}F_{xrr} + \frac{w}{2}F_{yfl}\sin\delta \\ -\frac{w}{2}F_{yfr}\sin\delta - l_r F_{yrl} - l_r F_{yrr} + l_f F_{yfl}\cos\delta + l_f F_{yfr}\cos\delta - l_f F_{xfl}\sin\delta \\ -l_f F_{xfr}\sin\delta + M_{zfl} + M_{zfr} + M_{zrl} + M_{zrr} \end{bmatrix} \tag{24}$$

where J_z is the moment of inertia around the z-axis. The roll and pitch motion depend very much on the longitudinal and lateral accelerations. Since only the vehicle body undergoes roll and pitch, the sprung mass, denoted by m_s has to be considered in determining the effects of handling on pitch and roll motions as the following:

$$\ddot{\phi} = \frac{-m_s c a_y + \phi\left(m_s gc - k_\varphi\right) + \dot{\phi}\left(-\beta_\phi\right)}{J_{sx}} \tag{25}$$

$$\ddot{\theta} = \frac{-m_s c a_y + \theta\left(m_s gc - k_\theta\right) + \dot{\theta}\left(-\beta_\theta\right)}{J_{sy}} \tag{26}$$

where c is the height of the sprung mass centre of gravity to the ground, g is the gravitational acceleration and k_ϕ, β_ϕ, k_θ and β_θ are the damping and stiffness constant for roll and pitch, respectively. The moments of inertia of the sprung mass around x and y-axis are denoted by J_{sx} and J_{sy} respectively.

2.4 Braking and throttling torques

For the front and rear wheels, the sums of the torque about the axis as shown in Figure 3 are as follows:

$$F_{xf} R_\omega - T_{bf} + T_{af} = I_\omega \dot{\omega}_f \tag{27}$$

$$F_{xr} R_\omega - T_{br} + T_{ar} = I_\omega \dot{\omega}_r \tag{28}$$

where ω_f and ω_r are the angular velocity of the front and rear wheels, I_ω is the inertia of the wheel about the axle, R_ω is the wheel radius, T_{bf} and T_{br} are the applied braking torques, and T_{af} and T_{ar} are the applied throttling torques for the front and rear wheels.

Figure 3 Free body diagram of a wheel

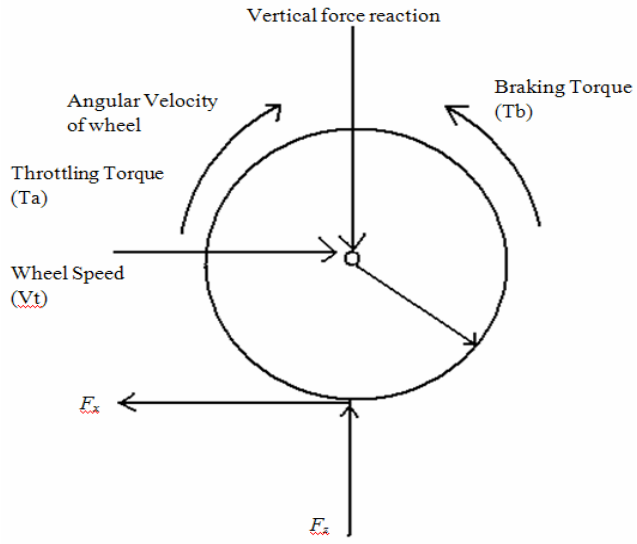

2.5 Simplified Calspan tyre model

Tyre model considered in this study is Calspan model as described in Szostak et al. (1988). Calspan model is able to describe the behaviour of a vehicle in any driving scenario including inclement driving conditions which may require severe steering, braking, acceleration, and other driving related operations (Kadir et al., 2008). The longitudinal and lateral forces generated by a tyre are a function of the slip angle and longitudinal slip of the tyre relative to the road. The previous theoretical developments in Szostak et al. (1988) lead to a complex, highly non-linear composite force as a function of composite slip. It is convenient to define a saturation function, *f(σ)*, to obtain a composite force with any normal load and coefficient of friction values (Singh et al., 2002). The polynomial expression of the saturation function is presented by:

$$f(\sigma) = \frac{F_c}{\mu F_z} = \frac{C_1\sigma^3 + C_2\sigma^2 + \left(\frac{4}{\pi}\right)\sigma}{C_1\sigma^3 + C_2\sigma^2 + C_4\sigma + 1} \tag{29}$$

where C_1, C_2, C_3 and C_4 are constant parameters fixed to the specific tyres. The tyre contact patch lengths are calculated using the following two equations:

$$ap_0 = \frac{0.0768\sqrt{F_z F_{ZT}}}{T_w\left(T_p + 5\right)} \tag{30}$$

$$ap = \left(1 - \frac{K_a F_x}{F_z}\right) \tag{31}$$

where *ap* is the tyre contact patch, T_w is a tread width, and T_p is a tyre pressure. The values of F_{ZT} and K_α are tyre contact patch constants. The lateral and longitudinal stiffness coefficients (K_s and K_c, respectively) are a function of tyre contact patch length and normal load of the tyre as expressed as follows:

$$K_s = \frac{2}{ap_0{}^2}\left(A_0 + A_1 F_z - \frac{A_1 F_z{}^2}{A_2}\right) \tag{32}$$

$$K_c = \frac{2}{ap_0{}^2} F_z\left(CS / FZ\right) \tag{33}$$

where the values of A_0, A_1, A_2 and *CS/FZ* are stiffness constants and can be found in Table 2. Then, the composite slip calculation becomes:

$$\sigma = \frac{\pi ap^2}{8\mu_0 F_z}\sqrt{K_s{}^2 \tan^2\alpha + K_c{}^2\left(\frac{s}{1-s}\right)^2} \tag{34}$$

μo is a nominal coefficient of friction and has a value of 0.85 for normal road conditions, 0.3 for wet road conditions, and 0.1 for icy road conditions. Given the polynomial saturation function, lateral and longitudinal stiffness, the normalised lateral and longitudinal forces are derived by resolving the composite force into the side slip angle and longitudinal slip ratio components:

$$\frac{F_y}{\mu F_z} = \frac{f(\sigma) K_s \tan\alpha}{\sqrt{K_s^{\,2} \tan^2\alpha + K_c^{'2} S^2}} + Y_\gamma \gamma \tag{35}$$

$$\frac{F_x}{\mu F_z} = \frac{f(\sigma) K_c^{'} S}{\sqrt{K_s^{\,2} \tan^2\alpha + K_c^{'2} S^2}} \tag{36}$$

Lateral force has an additional component due to the tyre camber angle, γ, which is modelled as a linear effect. Under significant manoeuvring conditions with large lateral and longitudinal slip, the force converges to a common sliding friction value. In order to meet this criterion, the longitudinal stiffness coefficient is modified at high slips to transition to lateral stiffness coefficient as well as the coefficient of friction defined by the parameter K_μ.

$$K_c^{'} = K_c + (K_s - K_c)\sqrt{\sin^2\alpha + S^2\cos^2\alpha} \tag{37}$$

$$\mu = \mu_0 (1 - K_\mu)\sqrt{\sin^2\alpha + S^2\cos^2\alpha} \tag{38}$$

2.6 Description of the simulation model

The vehicle dynamics simulation model was developed based on the mathematical equations presented in the previous section by using MATLAB SIMULINK software. The relationship between handling model, ride model, tyre model, slip angle and longitudinal slip are clearly described in Figure 4. In this model there are two inputs that can be used in the dynamic analysis of the vehicle namely torque input and steering input which come from driver. It simply explains that the model created is able to perform the analysis for longitudinal and lateral direction.

Figure 4 Full vehicle model in MATLAB SIMULINK

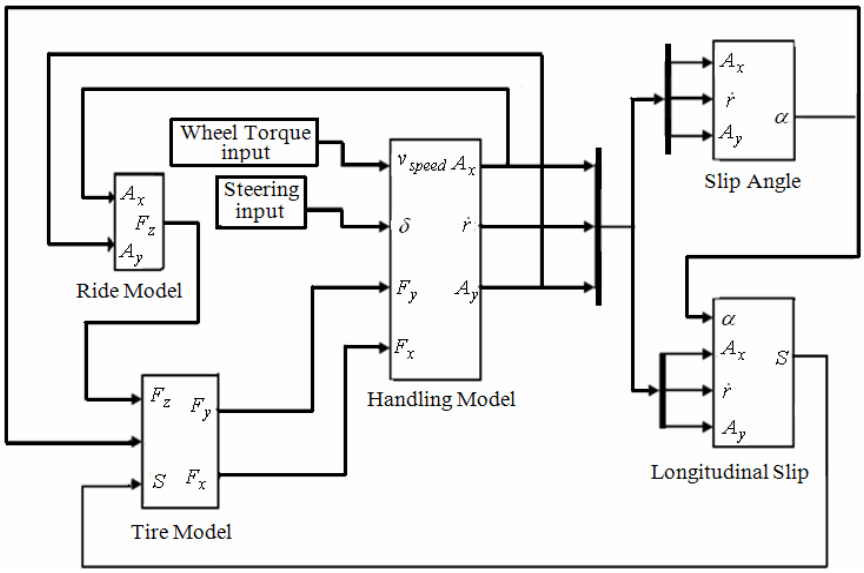

3 Active control system design

The controller structure consists of an inner loop controller to reject the unwanted weight transfer and an outer loop controller to stabilise heave and pitch responses due to pitch torque input from the driver. An input decoupling transformation is placed between inner and outer loop controllers that blend the inner loop and outer loop controllers. The outer loop controller provides the ride control that isolates the vehicle body from vertical and rotational vibrations induced by pitch torque input. The inner loop controller provides the weight transfer rejection control that maintains load-levelling and load distribution during vehicle manoeuvres. The proposed control structure is shown in Figure 5.

Figure 5 The proposed control structure for active suspension system

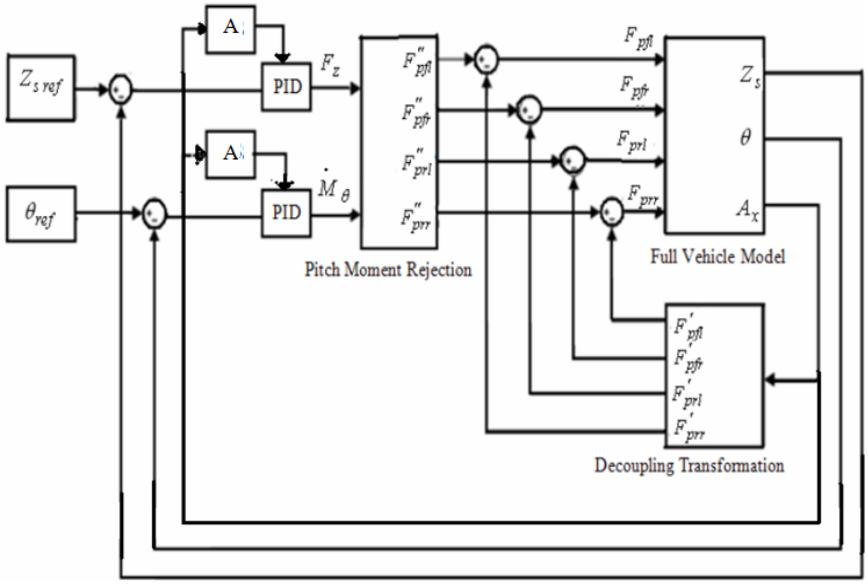

3.1 Decoupling transformation

The outputs of the outer loop controller are vertical forces to stabilise body bounce *(F_z)* and moment to stabilise pitch (M_θ). These forces and moments are then distributed into target forces of the four pneumatic actuators produced by the outer loop controller. Distribution of the forces and moments into target forces of the four pneumatic actuators is performed using decoupling transformation subsystem. The outputs of the decoupling transformation subsystem namely the target forces for the four pneumatic actuators are then subtracted with the relevant outputs from the inner loop controller to produce the ideal target forces for the four pneumatic actuators. Decoupling transformation subsystem requires an understanding of the system dynamics in the previous section. From equations (5), (6) and (7), equivalent forces and moments for heave, pitch and roll can be defined by:

$$F_z = F''_{pfl} + F''_{pfr} + F''_{prl} + F''_{prr} \tag{39}$$

$$M_\theta = -F''_{pfl} l_f - F''_{pfr} l_f + F''_{prl} l_r + F''_{prr} l_r \tag{40}$$

$$M_\phi = F''_{pfl}\left(\frac{w}{2}\right) - F''_{pfr}\left(\frac{w}{2}\right) + F''_{prl}\left(\frac{w}{2}\right) - F''_{prr}\left(\frac{w}{2}\right) \tag{41}$$

where $F''_{pfl}, F''_{pfr}, F''_{prl}$ *and* F''_{prr} are the pneumatic forces which are produced by outer loop controller in front left, front right, rear left and rear right corners, respectively. In the case of the vehicle input comes from brake torque, the roll moment can be neglected. Equations (39), (40) and (41) can be rearranged in a matrix format as the following:

$$\begin{bmatrix} F_z(t) \\ M_\theta(t) \\ M_\phi(t) \end{bmatrix} = \begin{bmatrix} 1 & 1 & 1 & 1 \\ -l_f & -l_f & l_r & l_r \\ \frac{w}{2} & -\frac{w}{2} & \frac{w}{2} & -\frac{w}{2} \end{bmatrix} \begin{bmatrix} F''_{pfl} \\ F''_{pfr} \\ F''_{prl} \\ F''_{prr} \end{bmatrix} \tag{42}$$

For a linear system of equations $\mathrm{y} = \mathrm{Cx}$, if $C \in \Re^{mxn}$ has full row rank, then there exists a right inverse C_1^{-1} such that $\mathrm{C}-1\,\mathrm{C} = 1^{mxm}$. The right inverse can be computed using $\mathrm{C}^{-1} = \mathrm{C}^T\left(\mathrm{CC}^T\right)^{-1}$. Thus, the inverse relationship of equation (42) can be expressed as:

$$\begin{bmatrix} F''_{pfl} \\ F''_{pfr} \\ F''_{prl} \\ F''_{prr} \end{bmatrix} = \begin{bmatrix} \frac{l_r}{2(l_f + l_r)} & -\frac{1}{2(l_f + l_r)} & \frac{1}{2w} \\ \frac{l_r}{2(l_f + l_r)} & -\frac{1}{2(l_f + l_r)} & -\frac{1}{2w} \\ \frac{l_f}{2(l_f + l_r)} & \frac{1}{2(l_f + l_r)} & \frac{1}{2w} \\ \frac{l_f}{2(l_f + l_r)} & \frac{1}{2(l_f + l_r)} & -\frac{1}{2w} \end{bmatrix} \begin{bmatrix} F_z \\ M_\theta \\ M_\phi \end{bmatrix} \tag{43}$$

3.2 Pitch moment rejection loop

In the outer loop controller, APID control is applied for suppressing both body vertical displacement and body pitch angle. The inner loop controller of pitch moment rejection control is described as follows: during throttling and braking, a vehicle will produce a force namely throttling force and braking force respectively at the body centre of gravity. The throttling force generates pitch moment causing the body centre of gravity to shift backward as shown in Figure 6 and vice versa when braking input is applied. Shifting the body centre of gravity causes a weight transfer from axle to the other axle. By defining the distance between the body centre of gravity and the longitudinal acceleration is A_x while the pitch pole is H_{pc}, pitch moment is defined by:

$$M_p = m\left(A_x\right) H_{pc} \tag{44}$$

In case of braking, the two pneumatic actuators installed in the front axle have to produce the necessary forces to cancel out the unwanted pitch moments, whereas the forces of the two pneumatic actuators at the rear axle will act in the opposite. Pneumatic forces that cancel out pitch moment in each corner due to braking input are defined as:

$$F'_{pfr} = F'_{pfl} = \frac{M_p(A_x)H_{pc}}{L_f} \text{ and } F'_{prl} = F'_{prr} = -\left[\frac{M_p(A_x)H_{pc}}{L_f}\right] \tag{45}$$

Whereas, pneumatic forces to cancel out pitch moment in each corner for throttle input can be defined as:

$$F'_{prl} = F'_{prr} = \frac{M_p(A_x)H_{pc}}{L_r} \text{ and } F'_{pfl} = F'_{pfr} = -\left(\frac{M_p(A_x)H_{pc}}{L_r}\right) \tag{46}$$

The ideal target forces for each pneumatic actuator are defined as the target forces produced by outer loop controller subtracted with the respective target forces produced by inner loop controller as the following:

$$F_{pfl} = F''_{pfl} - F'_{pfl} \tag{47}$$

$$F_{pfr} = F''_{pfr} - F'_{pfr} \tag{48}$$

$$F_{prl} = F''_{prl} - F'_{prl} \tag{49}$$

$$F_{prr} = F''_{prr} - F'_{prr} \tag{50}$$

Figure 6 Free body diagram for pitch motion

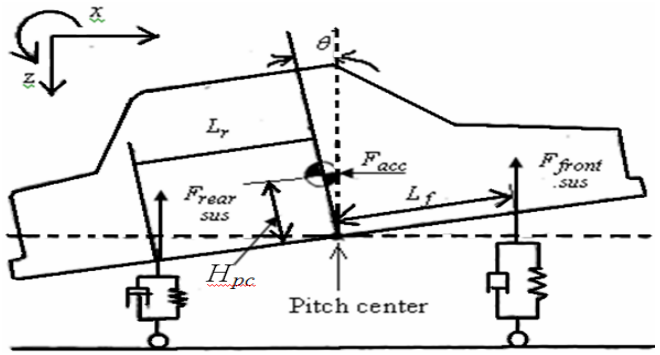

3.3 APID control

From many previous researches, it has been identified that PID controller is already proven effective in many applications but unable to continuously vary with variation condition. Because of that an APID controller is needed. The APID controller that is applied in the suspension system can be described by the following equation:

$$F_z(t) = K_p(t)\, e(t) + K_i(t)\int e(t)dt + K_d(t)\frac{d}{dt}e(t) \tag{51}$$

where $e(t) = Z_s ref(t) - Z_s(t)$ and the proportional gain $K_{p(t)}$, integral gain $K_{i(t)}$, and derivative gain $K_{d(t)}$, are the function of the position longitudinal acceleration $A_{x(t)}$. The proportional gain $K_{p(t)}$ as the function of the longitudinal acceleration $A_{x(t)}$ can be expressed mathematically as follows:

$$K_p(t) = 162.3A_x(t) + 2231 \tag{52}$$

The integral gain $k_{i(t)}$ in equation (51) as a function of position longitudinal acceleration $A_{x(t)}$ can be expressed mathematically as follows:

$$K_i(t) = -131.2\, A_x(t) + 720.6 \tag{53}$$

The derivative gain $k_{d(t)}$ in equation (51) as a function of longitudinal acceleration $A_{x(t)}$ can be expressed mathematically as follows:

$$K_d(t) = -106.0\, A_x(t) + 1660 \tag{54}$$

On the other hand the same function is used follows for stabilised body pitch and it can be expressed mathematically as follows:

$$M_\theta(t) = K_p(t)\, e(t) + K_i(t)\int e(t)dt + K_d(t)\frac{d}{dt}e(t) \tag{55}$$

where $e(t) = \theta_{ref}(t) - \theta(t)$ and the proportional gain $K_{p(t)}$, integral gain $K_{i(t)}$, and derivative gain $K_{d(t)}$, are the function of the position longitudinal acceleration $A_{x(t)}$, where the proportional gain $K_{p(t)}$ are:

$$K_p(t) = 121.2\, A_x(t) + 2015 \tag{56}$$

The integral gain $K_{i(t)}$ in equation (55) as a function of longitudinal acceleration $A_{x(t)}$ can be expressed mathematically as follows:

$$K_i(t) = -56.27\, A_x(t) + 243.7 \tag{57}$$

The derivative gain $K_{d(t)}$ in equation (55) as a function of longitudinal acceleration $A_{x(t)}$ can be expressed mathematically as follows:

$$K_d(t) = -133.6\, A_x(t) + 1261 \tag{58}$$

The constant values in the equations (51) to (58) are obtained from linearisation of the controller gain with the value of longitudinal acceleration as discuss in Appendix on Figure 12 and Figure 13. Before linearisation is made, it is necessary to identify the PID controller parameters of all the input condition in simulation of sudden acceleration and sudden braking test.

In these conditions the simulations have been made with 1Mpa, 3Mpa and 6Mpa brake pressure in sudden braking test, while 0.2, 0.6 and full step throttle for sudden acceleration test. The controller parameters that obtained from the tests are described in Table 1.

Table 1 PID controller parameters

Driver input	*Controller parameter*						*Longitudinal acceleration (G)* A_x
	Body displacement (controller for F_z)			*Body pitch (controller for M_θ)*			
	K_p	K_i	K_d	K_p	K_i	K_d	
1 Mpa brake	800	700	1,600	600	300	1,500	–1.36
3 Mpa brake	1,000	1,000	2,000	1,000	500	2,000	–2.72
6 Mpa brake	2,000	2,000	3,000	1,852	7,000	2,251	–8.2
0.2 step throttle	3,000	100	500	2,500	50	700	0.96
0.6 step throttle	1,000	900	750	2,700	57	800	2.89
Full step throttle	5,000	100	2,500	30,000	60	8,000	4.8

4 Validation of 14 DOF vehicle model using instrumented experimental vehicle

To verify the full vehicle ride and handling model that has been derived, experimental works were performed using an instrumented experimental vehicle. This section provides the verification of ride and handling model using visual technique by simply comparing the trend of simulation results with experimental data using the same input signals. Validation or verification is defined as the comparison of model's performance with the real system. Therefore, the validation does not meant the fitting of simulated data exactly to the measured data, but as gaining confidence that the vehicle handling simulation is giving insight into the behaviour of the simulated vehicle reference. The tests data are also used to check whether the input parameters for the vehicle model are reasonable. In general, model validation can be defined as determining the acceptability of a model by using some statistical tests for deviance measures or subjectively using visual techniques reference.

4.1 Vehicle instrumentation

The data acquisition system (DAS) was installed into the experimental vehicle to obtain the real vehicle reaction as to evaluate the vehicle's performance in terms of longitudinal acceleration, body vertical acceleration and pitch rate. The DAS uses several types of transducers such as single axis accelerometer to measure the sprung mass and unsprung mass accelerations for each corner, tri-axial accelerometer to measure longitudinal, vertical and lateral accelerations at the body centre of gravity, tri-axial gyroscopes for the pitch rate and wheel speed sensor to measure angular velocity of the tyre. The multi-channel μ-MUSYCS system integrated measurement and control (IMC) is used as the DAS system. Online FAMOS software as the real time data processing and display function is used to ease the data collection. The installation of the DAS and sensors to the experimental vehicle can be seen in Figure 7.

Figure 7 In-vehicle instrumentations (see online version for colours)

4.2 Experimental vehicle

An instrumented experimental vehicle was developed to validate the full vehicle model. A Malaysian National car was used to perform sudden braking and sudden acceleration test. Note that the vehicle is a 1,300 cc and used manual gear shift as the power terrain systems. The technical specifications of the vehicle are listed in Table 2.

Table 2 Experimental vehicle parameter

Parameter	*Value*
Vehicle mass	920 kg
Wheel base	2,380 mm
Wheel track	1,340 mm
Spring rate: front: rear:	30 N/mm 30 N/mm
Damper rate: front: rear	1,000 N/msec^{-1} 1,000 N/msec^{-1}
Roll centre	100
Centre of gravity	550 mm
Wheel radius	285 mm

4.3 Validation procedures

The dynamic response characteristics of a vehicle model that include longitudinal acceleration, longitudinal slip in each tyre and pitch rate can be validated using

experimental test through several handling test procedures namely sudden braking test and sudden acceleration test. Sudden braking test is intended to study transient response of the vehicle under braking input. In this case, the tests were conducted by accelerating the vehicle to a nominal speed of 60 kph and activating the instrumentation package. The driver then applies the brake pedal hard enough to hold the pedal firmly until the vehicle stopped completely as shown in Figure 8(a). On the other hand, sudden acceleration test is used to evaluate the characteristics of the vehicle during a sudden increase of speed. In this study, the vehicle accelerated to a nominal speed of 40kph and activated the instrument package. The driver then manually applied the throttle pedal full step as required to make the vehicle accelerated immediately as shown in Figure 8(b).

Figure 8 Response of the vehicle for sudden braking test at 60 kph constant speed, (a) vehicle speed (b) longitudinal speed (c) pitch rate (d) longitudinal slip front right (e) longitudinal slip front left (f) longitudinal slip rear left (g) longitudinal slip rear right

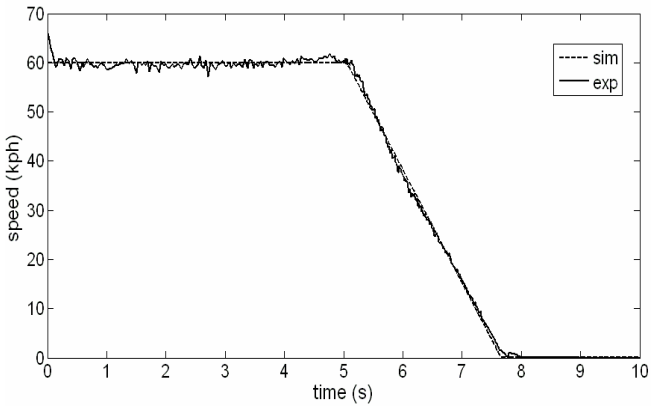

(a)

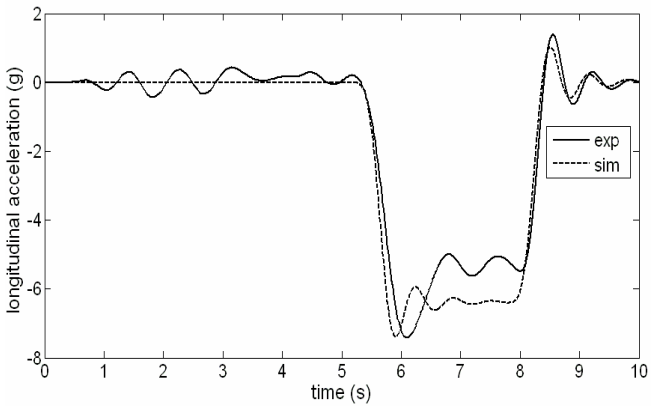

(b)

Figure 8 Response of the vehicle for sudden braking test at 60 kph constant speed, (a) vehicle speed (b) longitudinal speed (c) pitch rate (d) longitudinal slip front right (e) longitudinal slip front left (f) longitudinal slip rear left (g) longitudinal slip rear right (continued)

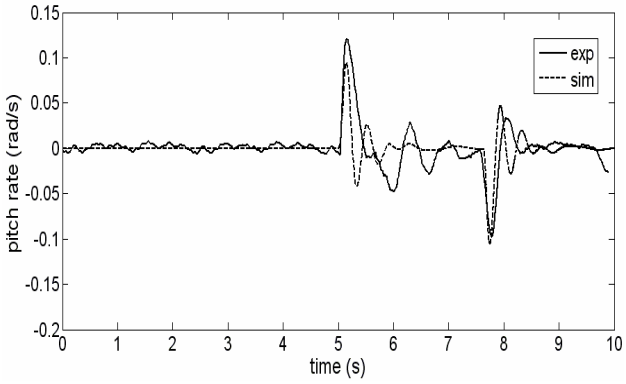

(c)

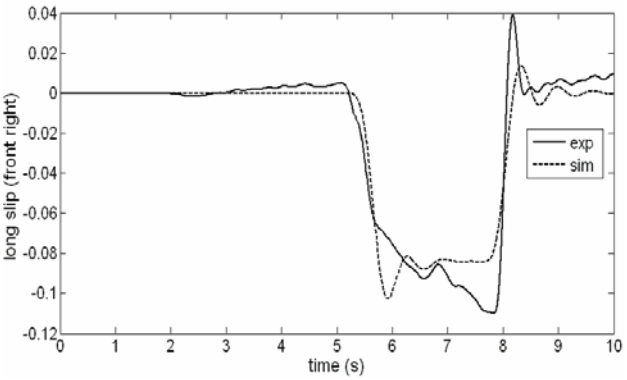

(d)

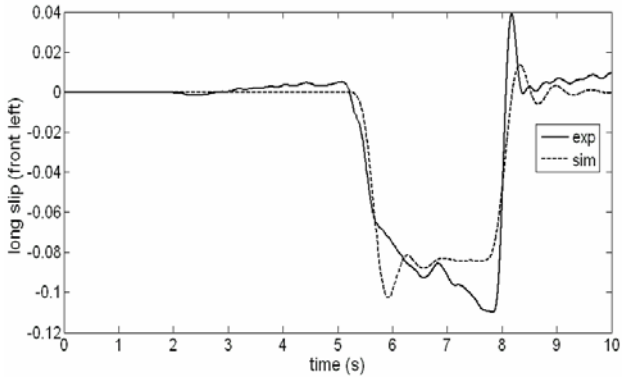

(e)

Figure 8 Response of the vehicle for sudden braking test at 60 kph constant speed, (a) vehicle speed (b) longitudinal speed (c) pitch rate (d) longitudinal slip front right (e) longitudinal slip front left (f) longitudinal slip rear left (g) longitudinal slip rear right (continued)

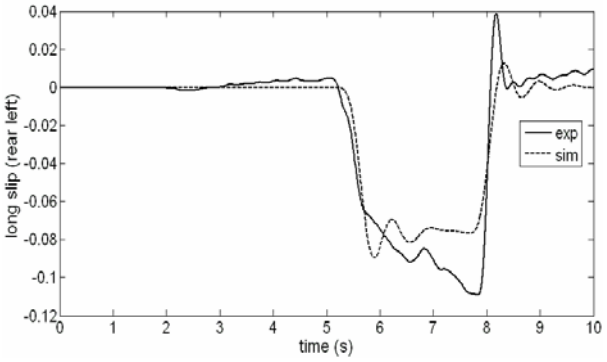

(f)

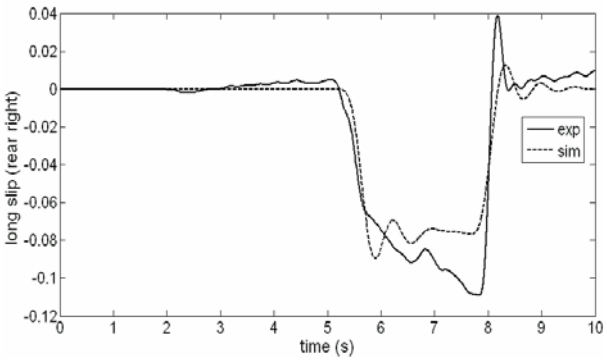

(g)

4.4 Validation results

Figures 8 and 9 show a comparison of the results obtained using SIMULINK and experimental. In experimental works, all the experimental data are filtered to remove out any unintended data. It is necessary to note that the measured vehicle speed from the speed sensor is used as the input of simulation model. For the simulation model, tyre parameters are obtained from Szostak et al. (1988) and Singh et al. (2002). The results of model verification for sudden braking test at 60 kph are shown in Figure 8. Figure 8(a) shows the vehicle speed applied for the test. It can be seen that the trends between simulation results and experimental data are almost similar with acceptable error. The small difference in magnitude between simulation and experimental results is due to the fact that, in an actual situation, it is indeed very hard for the driver to maintain the in a perfect speed as compared to the result obtained in the simulation.

In terms of both longitudinal acceleration and pitch rate response, it can be seen that there are quite good comparisons during the initial transient phase as well as during the following steady state phase as shown in Figures 8(b) and (c) respectively. Longitudinal slip responses of the front tyres also show satisfactory matching with only small

deviation in the transition area between transient and steady state phases as shown in Figure 8(d) and (e). It can also be noted that the longitudinal slip responses of all tyres in the experimental data are slightly higher than the longitudinal slip data obtained from the simulation responses particularly for the rear tyres as can be seen in Figures 8(f) and (g). This is due to the fact that it is difficult for the driver to maintain a constant speed during manoeuvring. In simulation, it is also assumed that the vehicle is moving on a flat road during step steer manoeuvre. In fact, it is observed that the road profiles of test field consist of irregular surface. This can be another source of deviation on longitudinal slip response of the tyres.

The results of sudden acceleration test at constant speed of 40 kph indicate that measurement data and the simulation results agree with a relatively good accuracy as shown in Figure 9. Figure 9(a) shows the vehicle speed which is used as the input for the simulation model. In terms of pitch rate and longitudinal acceleration, it can be seen clearly that the simulation and experimental result are very similar with minor difference in magnitude as shown in Figures 9(b) and (c). The minor difference in magnitude and small fluctuation occurred on the measured data is due to the body flexibility which was ignored in the simulation model. In terms of tyre longitudinal slip, the trends of simulation results show close agreement for both experimental data and simulation and shown in Figures 9(d), (e), (f) and (g). Closely similar to the validation results obtained from sudden acceleration test, the longitudinal responses of all tyres in experimental data are smaller than the longitudinal slip data obtained from the simulation. Again, this is due to the difficulty of the driver to maintain a constant speed during sudden acceleration test manoeuvre. Assumption in simulation model that the vehicle is moving on a flat road during the manoeuvre is also very difficult to realise in practice. In fact, road irregularities of the test field may cause the change in tyre properties during vehicle handling test. Assumption of neglecting steering inertia may be possibility in lowering down the magnitude of tyre longitudinal slip in simulation results compared with the measured data.

Figure 9 Response of the vehicle for sudden acceleration test at constant speed 40 kph, (a) vehicle speed (b) longitudinal speed (c) pitch rate (d) longitudinal slip front right (e) longitudinal slip front left (f) longitudinal slip rear left (g) longitudinal slip rear right

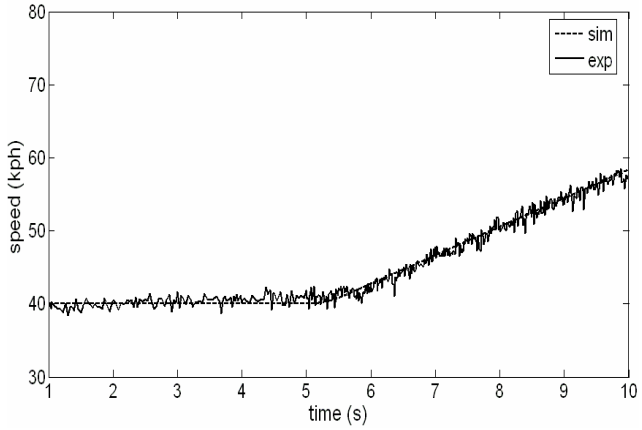

(a)

Figure 9 Response of the vehicle for sudden acceleration test at constant speed 40 kph, (a) vehicle speed (b) longitudinal speed (c) pitch rate (d) longitudinal slip front right (e) longitudinal slip front left (f) longitudinal slip rear left (g) longitudinal slip rear right (continued)

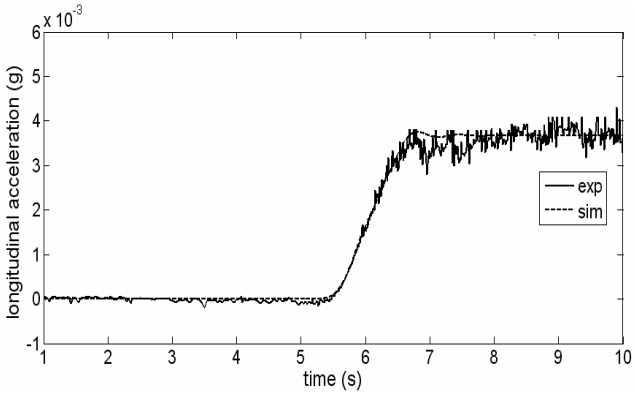

(b)

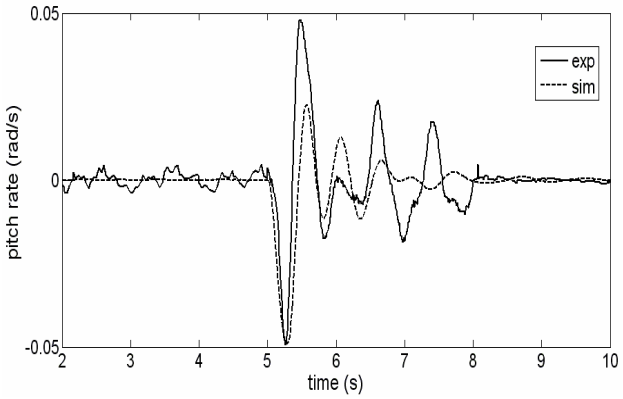

(c)

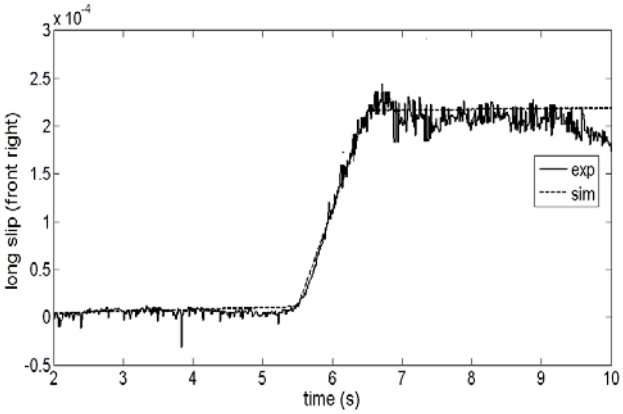

(d)

Figure 9 Response of the vehicle for sudden acceleration test at constant speed 40 kph, (a) vehicle speed (b) longitudinal speed (c) pitch rate (d) longitudinal slip front right (e) longitudinal slip front left (f) longitudinal slip rear left (g) longitudinal slip rear right (continued)

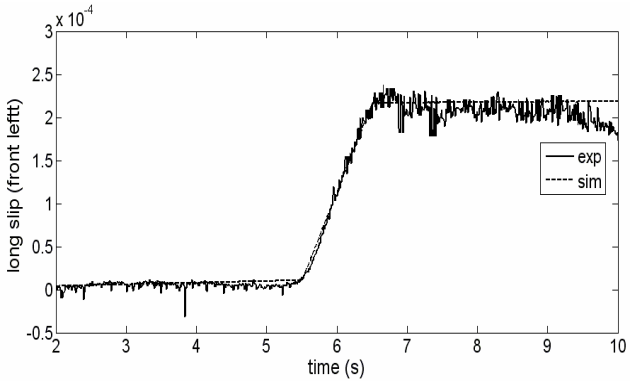

(e)

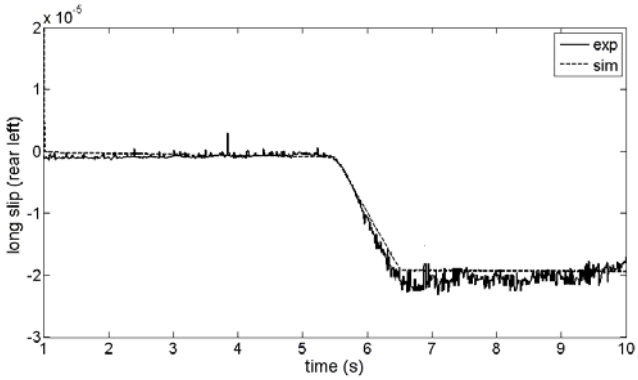

(f)

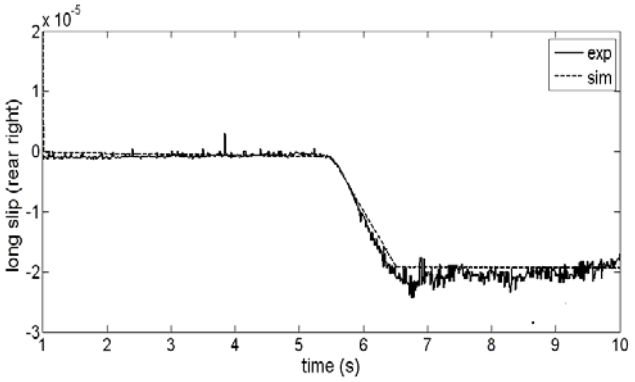

(g)

5 Performance evaluation of APID control

The performance of APID controller is examined through simulation studies using SIMULINK toolbox of the MATLAB software package. For comparison purposes, the performance of the GSPID is compared with both the conventional PID control approach and passive system. The performance of the controller is examined through vehicle translational motion namely body pitch angle, pitch rate, body acceleration and body displacement.

5.1 Simulation parameters

The simulation study was performed for a period of 10 seconds using Heun solver with a fixed step size of 0.01 second. The controller parameters were obtained using trial and error technique. The numerical values of the 14-DOF full vehicle model parameters and Calspan tyre model parameters as well as the controller parameters are as Table 3.

Table 3 Tyre parameter

Parameter	*FWD radial*
Tyre designation	P185/70R13
T_w	7.3
T_p	24
F_{ZT}	980
C_1	1.0
C_2	0.34
C_3	0.57
C_4	0.32
A_o	1,068
A_1	11.3
A_2	2,442.73
A_3	0.31
A_4	–1,877
K_a	0.05
CS/FZ	17.91
μ_o	0.85

5.2 Step change test driver input

To study the performance of APID controller, a step function driver input test is applied. The tests consist of sudden braking test and sudden acceleration test. In sudden braking test, the vehicle was accelerated and maintained to a nominal speed of 70 kph, then 6 MPa brake is applied to hold the pressure firmly until the vehicle stopped completely. For the remainder of the simulation, the steering is maintained constantly at zero degree appropriately. In sudden acceleration test the same condition was applied to the vehicle,

and then full step throttle input was applied to make the vehicle accelerates immediately. In order to fulfil the objective of designing the active suspension system, there are four parameters observed in the simulations. The four parameters are the vehicle body acceleration, body displacement, pitch rate and pitch angle. In the results presented solid lines represent as the active suspension under APID controller, the dashed lines represent as the active suspension under PID controller and the dotted lines for the passive system response.

From Figures 10(a) and (b), the pitch behaviour for the APID controller indicates better performance reduced dive during the manoeuvre compared to conventional PID. It is shown in the vertical acceleration plot. The APID made the vehicle lose the momentum during the manoeuvres and reduced the vehicle weight transfer to the front. Figure 10(c) illustrates clearly how the APID can effectively absorb the vehicle vibration in comparison to active suspension under PID controller and the passive suspension system. The oscillation of the body acceleration using the APID system is much reduced significantly, which guarantees better ride comfort and reduced the body vertical displacement as shown in Figure 10(d).

Figure 10 Performance of GSPID at step function brake 6 MPa, (a) pitch angle (b) pitch rate (c) body acceleration (d) body displacement

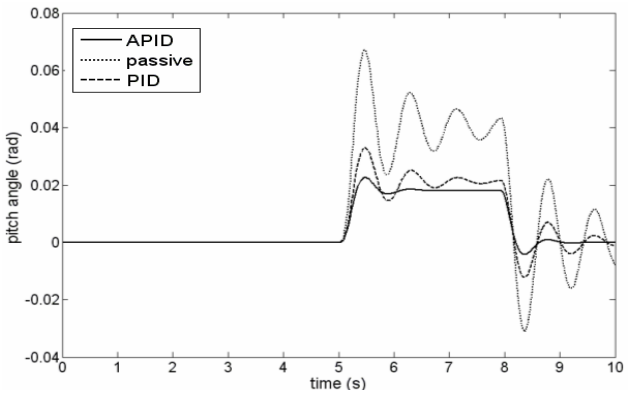

(a)

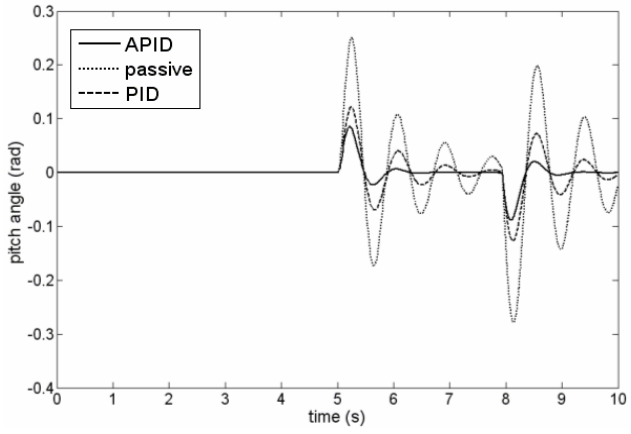

(b)

Figure 10 Performance of GSPID at step function brake 6 MPa, (a) pitch angle (b) pitch rate (c) body acceleration (d) body displacement (continued)

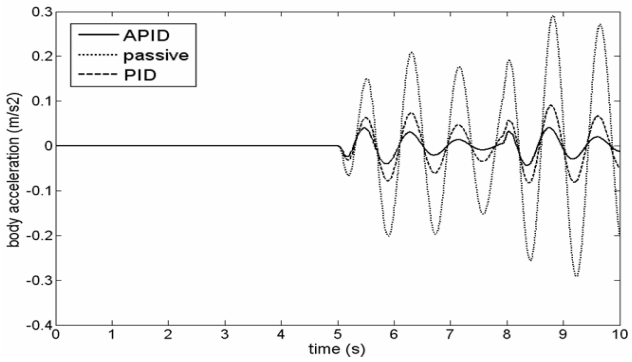

(c)

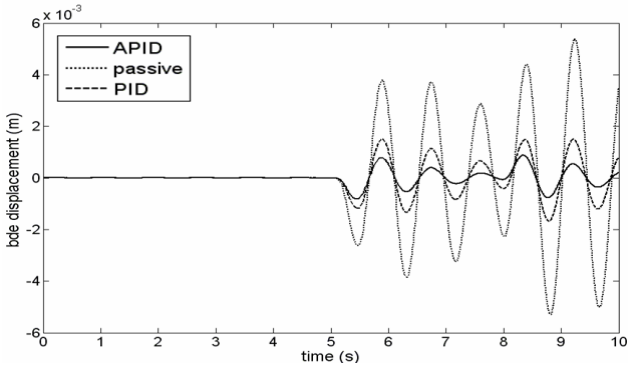

(d)

Figure 11 Performance of GSPID at step function full throttle, (a) pitch angle (b) pitch rate (c) body acceleration (d) body displacement

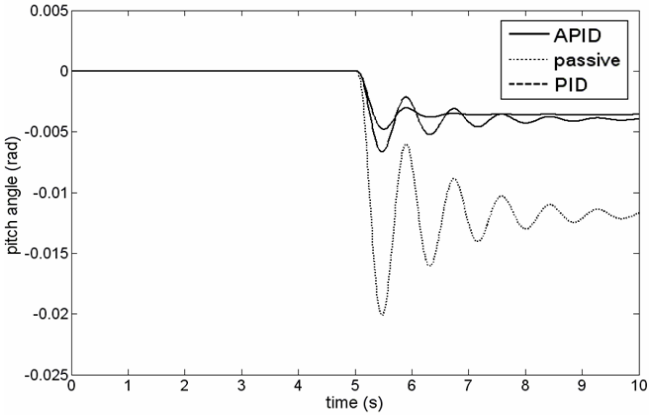

(a)

Figure 11 Performance of GSPID at step function full throttle, (a) pitch angle (b) pitch rate (c) body acceleration (d) body displacement (continued)

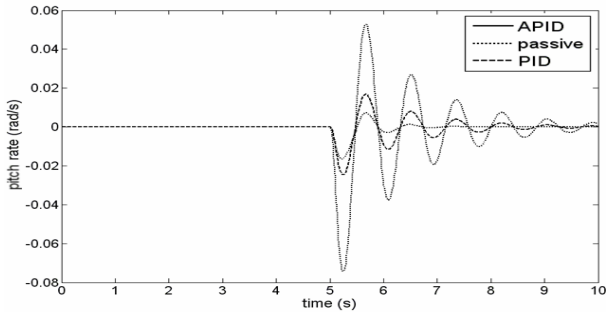

(b)

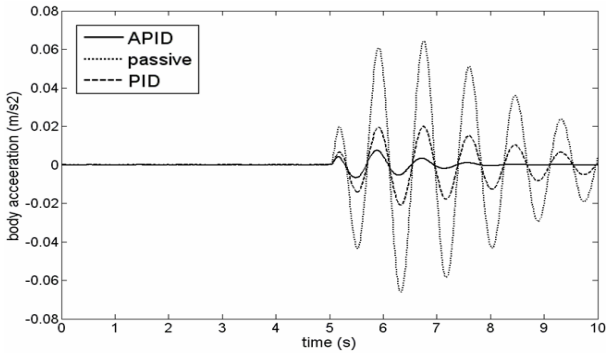

(c)

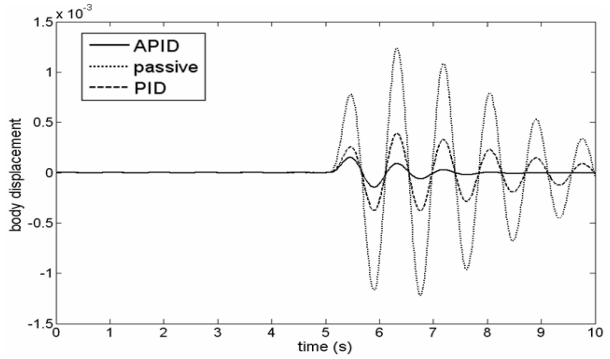

(d)

The results of the sudden acceleration test show that the proposed controllers, APID are reasonably efficient method in enhancing vehicle stability in terms of reducing squat. In this case the input of the vehicle is changed from braking to throttling input. Figure 11 shows that performance of APID controller which has a good tracking performance with good transient response. Figure 11 (a) shows the response of the vehicle from sudden acceleration test manoeuvre which is input for the simulation model. In terms of pitch rate the proposed controller gives the system output more stable when it is compared with PID structures as shown in Figure 11 (b). The result of the body acceleration and body

displacement are shown in Figures 11 (c) and Figure 11 (d) respectively. The figure explained that the APID controller gives the better performance in term of settling time and reducing the magnitude as compared to the counterparts.

6 Conclusions

An APID controller with pitch moment rejection for vehicle dive and squat to enhance vehicle stability and ride quality has been evaluated. The proposed controller includes proportional, integral and derivative gains that are allowed to vary within predetermined range of the sudden braking and sudden acceleration tests. Simulation studies for an active suspension with validated full vehicle model are presented to demonstrate the effectiveness of using the APID controller. Two types of simulation tests namely sudden braking test and sudden acceleration test have been performed and data gathered from the tests were used as the benchmark of the proposed verification. Some of the vehicle's behaviours observed in these works are pitch rate, pitch angle, body acceleration and body displacement responses. The performance characteristics of the controller are evaluated and compared with conventional PID. The result shows that the use of the proposed APID control technique proved to be effective in controlling vehicle pitch and vibration and achieve better performance than the conventional PID controller.

Acknowledgements

This work is supported by the Ministry of Science Technology and Innovation (MOSTI) through it scholarship and financial support and Ministry of Higher Education (MoHE) of Malaysia through FRGS project entitled 'Development of a Pneumatically Actuated Active Stabilizer Bar to Reduce Unwanted Motion In Longitudinal Direction' lead by Dr. Khisbullah Hudha at the Universiti Teknikal Malaysia Melaka. This financial support is gratefully acknowledged.

References

Ahmad, F., Hudha, K. and Harun, M.H. (2009) 'Pneumatically actuated active suspension system for reducing vehicle dive and squat', *Jurnal Mekanikal UTM*, No. 28, pp.85–114.

Ahmad, F., Hudha, K., Said, M.R. and Rivai, A. (2008a) 'Development of pneumatically actuated active stabilizer bar to reduce vehicle dive', *Proceedings of the International Conference Plan Equipment and Reliability*, 27–28 March, Kuala Lumpur, Malaysia.

Ahmad, F., Hudha, K., Said, M.R. and Rivai, A. (2008b) 'Development of pneumatically actuated active stabilizer bar to reduce vehicle squat', *Proceedings of the 3rd Brunei International Conference on Engineering and Technology 2008*, 2–5 November, Bandar Sri Begawan, Brunei Darussalam.

Alleyne, A. and Hedrick, J.K. (1995) 'Nonlinear adaptive control of active suspensions', *IEEE Transaction on Control System Technology*, Vol. 3, No. 1, pp.94–101.

Bahouth, G. (2005) 'Real world crash evaluation of vehicle stability control (VSC) technology', *49th Annual Proceedings Association for the Advancement of Automotive Medicine*, 12–14 September, Boston, Massachusetts, USA.

Campos, J., Davis, L., Lewis, F., Ikanega, S., Scully, S. and Evans, M. (1999) 'Active suspension system control of ground vehicle heave and pitch motions', *Proceedings of the 7th IEEE Mediterranean Control Conference on Control and Automation*, 28–30 June, Haifa, Israel.

DeCarlo, R.A., Zak, S.H. and Matthews, G.P. (1988) 'Variable structure control of nonlinear multivariable system: a tutorial', *Proceedings of the IEEE*, Vol. 76, No. 3, pp.212–232.

Fenchea, M. (2008) 'Influence of car's suspension in the vehicle comfort and active safety', *Annals of the University of Oradea, Fascicle of Management and Technology Engineering*, Vol. 7, No. 17, pp.791–796.

Fialho, I. and Balas, G.J. (2002) 'Road adaptive active suspension design using linear parameter varying gain-scheduling', *IEEE Transactions on Control System Technology*, Vol. 10, No. 1, pp.43–51.

Fischer, D. and Isermann, R. (2004) 'Mechatronic semi-active and active vehicle suspensions', *Control Engineering Practice*, Vol. 12, pp.1353–1367.

Gao, B., Darling, J., Tilley, D.G. and Williams, R.A. (2006) 'Modeling and simulation of a semi-active suspension system', Department of Mechanical Engineering, University of Bath, Bath a.d Engineering Centre, Jaguar and Land Rover, Whitely, Coventry, UK.

Garg, D.P. and Kumar, M. (2002) 'Optimal path planning and torque minimization via genetic algorithm applied to cooperating robotic manipulators', *American Society of Mechanical Engineers, Dynamic Systems and Control Division DSC*, Vol. 70, 17–22 November, New Orleans, Louisiana, USA, pp.71–79.

Holford, K.M., Margaret, K., Surawattanawan, P. and Watton, J. (2001) 'Electrohydraulic effects on the modelling of a vehicle active suspension', *Proceedings of the Institution of Mechanical Engineers, Part D: Journal of Automobile Engineering*, Vol. 215, No. 10, pp.1077–1092.

Hrovat, D. (1991) 'Optimal active suspension for 3D vehicle models', *American Control Conference*, 26–28 June, Boston, Massachusetts, USA.

Hudha, K., Jamaluddin, H., Samin, P.M. and Rahman, R.A. (2003) 'Semi active roll control suspension system on a new modified half car model' SAE Technical Paper Series, Paper No. 2003-01-2274.

Hudha, K., Kadir, Z., Jamaluddin, H. and Said, M.R. (2009) 'Modeling, validation and roll moment rejections control for pneumatically actuated active roll control for improving vehicle lateral dynamics performance', *International Journal Engineering System Modeling and Simulation (IJESMS)*, Vol. 1, Nos. 2/3, pp.122–136.

Ikanega, S., Lewis, F.L., Campos, J. and Davis, L. (2000) 'Active suspension control of ground vehicle based on a full-vehicle model', *Proceeding of the American Control Conference on Ground Vehicle Based*, 28–30 June, Chicago, Illinois, USA, Vol. 6, pp.4019–4024.

Kadir, Z.A., Hudha, K., Nasir, M.Z.M. and Said, M.R. (2008) 'Assessment of tyre models for vehicle dynamics analysis', *Proceedings of the International Conference on Plant Equipment and Reliability*, 27–28 March, Kuala Lumpur, Malaysia.

Karnopp, D. (1995) 'Active and semi-active vibration isolation', *Journal of Mechanical Design, ASME*, Vol. 177, pp.177–185.

Kasprzak, E.M. and Gentz, D. (2006) 'The formula SAE® tyre testing consortium – tyre testing and data handling', SAE Technical Paper. (2006-01-3606).

Kasprzak, E.M., Lewis, K.E. and Milliken, D.L. (2006) 'Modeling tyre inflation pressure effects in the nondimensional tyre model', SAE Technical Paper, Paper No. (2006-01-3607).

Kruczek, A. and Stribrsky, A. (2004) 'A full-car model for active suspension – some practical aspects', *Proceedings of the IEEE International Conference on Mechatronics*, 3–5 June, Istanbul Turkey, pp.41–45.

Lee, C.H., Shin, M.H. and Chung, N.J. (2001) 'A design of gain-scheduled control for a linear parameter varying system: an application to flight control', *Control Engineering Practice*, Vol. 9, pp.11–21.

Lin, J.S. and Kanellakopoulos, I. (1997) 'Nonlinear design of active suspension', *Proceedings of IEEE Control System Magazine*, Vol. 17, pp.1–26.

Mailah, M. and Priyandoko, G. (2007) 'Simulation of a suspension system with adaptive fuzzy active force control', *International Journal of Simulation Modeling*, Vol. 6, No. 1, pp.25–36.

March, C. and Shim, T. (2007) 'Integrated control of suspension and front steering to enhance vehicle handling', *Proc. IMechE. Journal of Automobile Engineering*, Vol. 221, No. 152, pp.377–391.

Park, J.H., and Kim, Y.S. (1998) 'Decentralized variable structure control for active suspensions based on a full-car model', *Proceeding of IEEE. International Conference on Control Applications*, 1–4 September, Trieste, Italy, pp.383–387.

Priyandoko, G. and Mailah, M. (2005) 'Fuzzy logic artificial neural network active force control for an active suspension of a quarter car', *Proceeding of ROVISP05*, USM Penang, 20–25 July.

Ruotsalainen, P., Nevala, K. and Marjanen, Y. (2006) 'Design of an adjustable hydro-pneumatic damper for cab suspension', *The Thirteenth International Congress on Sound and Vibration*, 2–6 July, Vienna Austria.

Sam, Y.M. and Osman, J.H.S (2005) 'Modeling and control of the active suspension system using proportional integral sliding mode approach', *Asian Journal of Control*, Vol. 7, No. 2, pp.91–98.

Sam, Y.M. and Osman, J.H.S. (2006) 'Sliding mode control of a hydraulically actuated active suspension', *Jurnal Teknologi*, Vol. 3, No. 44, pp.37–48.

Sam, Y.M., Ghani, M.R.H.A. and Ahmad, N. (2000) 'LQR controller for active suspension', *Proceeding of IEEE Conferences on TENCON 2000*, 24–27 September, Kuala Lumpur, Malaysia, Vol. 1, pp.441–444.

Sampson, D.J.M. (2002) 'Active roll control of articulated heavy vehicles, technical report CUED/C-MECH/TR 82', Department of Engineering, University of Cambridge, UK.

Sampson, D.J.M. and Cebon, D. (2003a) 'Achievable roll stability of heavy road vehicles', *Proc. Instn Mech. Engrs, Part: J. Automobile Engineering*, Vol. 217, No. 4, pp.269–287.

Sampson, D.J.M. and Cebon, D. (2003b) 'Active roll control of single unit heavy road vehicles', *Vehicle System Dynamics*, Vol. 40, No. 4, pp.229–270.

Sampson, D.J.M., Jeppesen, B.P. and Cebon, D. (2000) 'The development of an active roll control system for heavy vehicles, in *Proceedings of 6th International Symposium on Heavy Vehicle Weights and Dimensions*, 18–22 June, Saskatoon, Saskatchewan, Canada, pp.375–384.

Sedaghati, A. (2006) 'A PI controller based on gain-scheduling for synchronous generator', *Turkish Journal of Electrical Engineering and Computer Sciences*, Vol. 14, No. 2, pp.241–251.

Singh, T., Kesavadas, T., Mayne, R., Kim, J.J. and Roy, A. (2002) 'Design of hardware/algorithms for enhancement of driver-vehicle performance in inclement weather conditions using a virtual environment', *SAE 2004 Transactions Journal of Passenger Car: Mechanical Systems*, Paper No. 2002-01-0322.

Stilwell, D.J. and Rugh, W.J. (1999) 'Interpolation of observer state feedback controllers for gain scheduling', *IEEE Transactions on Automatic Control*, Vol. 44, No. 6, pp.1225–1229.

Su, J., Ordys, A. and Panahi, P. (2008) 'LQR-based linear controller of active suspension on a half-body model for improved ride comfort', *23rd IAR Workshop on Advanced Control and Diagnosis*, 27–28 November, Coventry University, UK.

Szostak, H.T., Allen, W.R. and Rosenthal, T.J. (1988) 'Analytical modeling of driver response in crash avoidance maneuvering volume II: an interactive model for driver/vehicle simulation, US Department of Transportation Report NHTSA DOT HS-807-271.

Ting, C.S., Li, T.H. and Kung, F.C. (1995) 'Design of fuzzy controller for active suspension system', *International Journal of Mechatronics*, Vol. 5, No. 4, pp.365–383.

Toshio, Y. and Itaru, T. (2005) 'Active suspension control of a one-wheel car model using single input rules modules fuzzy reasoning and a disturbance observer', *Journal of Zheijiang University SCIENCE*, Vol. 6A, No. 4, pp.251–256.

Vaughan, J., Singhose, W. and Sadegh, N. (2003) 'Use of active suspension control to counter the effects of vehicle payloads', *Proceeding of IEEE Conference on Control Applications, 2003 Istanbul, (CCA 2003)*, 23–25 June, Istanbul, Turkey, Vol. 1, pp.285–289.

Wang, F.C. and Smith, M.C. (2002) 'Active and passive suspension control for vehicle dive and squat', in Johansson, R. and Rantzer, A. (Eds.): *Nonlinear and Hybrid Systems in Automotive Control*, pp.23–39, Springer-Verlag, London, UK.

Weeks, D.A., Beno, J.H., Guenin, A.M. and Breise, D.A. (2000) 'Electromechanical active suspension demonstration for off road vehicles', SAE Technical Paper Series, Vol. 01, No. 0102.

Yoshimura, T. and Watanabe, K. (2003) 'Active suspension of a full car model using fuzzy reasoning based on single input rule modules with dynamic absorbers', *International Journal of Vehicle Design*, Vol. 31, No. 1, pp.22–40.

Yoshimura, T., Hiwa, T., Kurimoto, M. and Hino, J. (2003) 'Active suspension of a one-wheel car model using fuzzy reasoning and compensators', *International Journal of Vehicle Autonomous Systems*, Vol. 1, No. 2, pp.196–205.

Yoshimura, T., Isari, Y., Li, Q. and Hino, J. (1997a) 'Active suspension of motor coaches using skyhook damper and fuzzy logic controls', *Control Engineering Practice*, Vol. 5, No. 2, pp.175–184.

Yoshimura, T., Nakaminami, K. and Hino, J. (1997b) 'A semi-active suspension with dynamic absorbers of ground vehicles using fuzzy reasoning', *International Journal of Vehicle Design*, Vol. 18, No. 1, pp.19–34.

Yoshimura, T., Kume, A., Kurimoto, M. and Hino, J. (2001) 'Construction of an active suspension system of a quarter car model using the concept of sliding mode control', *Journal of Sound and Vibration*, Vol. 239, No. 2, pp.187–199.

Zhang, Y., Zhao, L., Cong, H. and Wang, B. (2004) 'Study on control of vehicle attitude and ride comfort based on full-car model', *Fifth World Congress on Intelligent Control and Automation, 2004, (WCICA 2004)*, 15–19 June, Hangzhou, China, Vol. 4, pp.3514–3519.

Appendix

Figure 12 Controller parameters for body bounce *(F_z)*, (a) Kp value (b) Ki value (c) Kd value (see online version for colours)

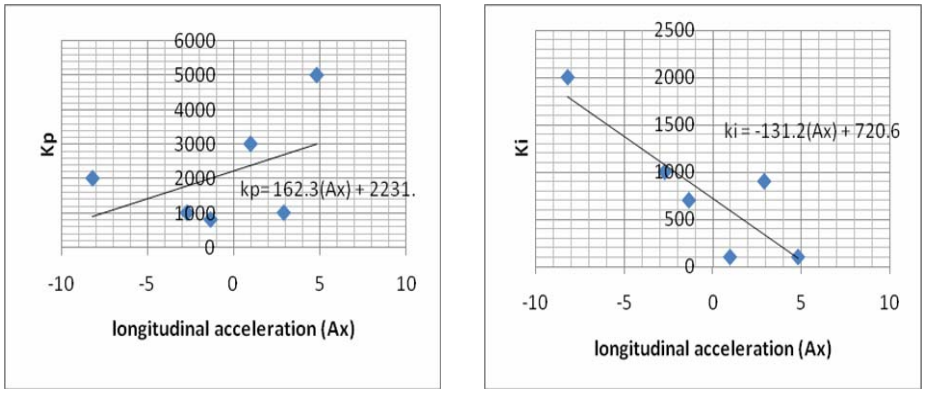

(a) (b)

Figure 12 Controller parameters for body bounce *(F_z)*, (a) Kp value (b) Ki value (c) Kd value (continued) (see online version for colours)

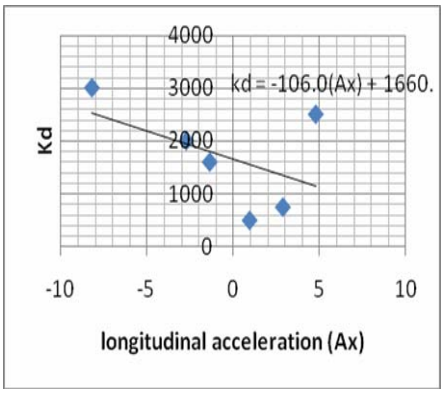

(c)

Figure 13 Controller parameters for body pitch *(M_θ)* (a) Kp value (b) Ki value (c) Kd value (see online version for colours)

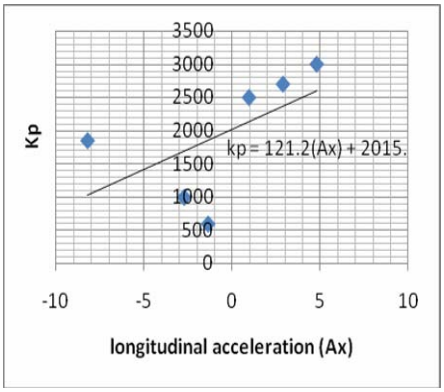

(a)

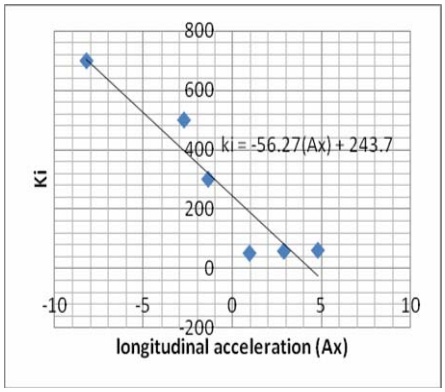

(b)

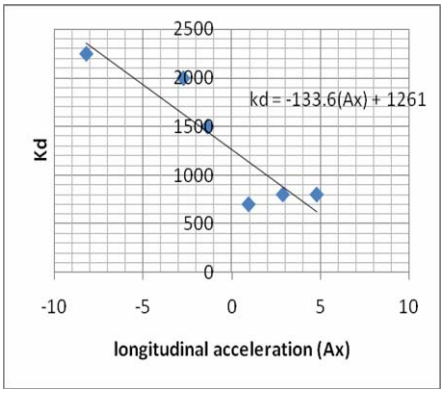

(c)